

Multi-sample micro-slit rheometry

Doyoung Moon,^{a)} Anthony J. Bur, and Kalman B. Migler

*Polymers Division, National Institute of Standards and Technology,
Gaithersburg, Maryland 20899*

(Received 14 December 2007; final revision received 2 June 2008)

Synopsis

We have developed a multi-sample micro-slit rheometer (MMR) which is capable of measurements over a broad range of temperatures, viscosities and shear rates. The instrument is mechanically simple as the flow is generated by external gas pressure and the shear rate is measured through optical tracking of the flow front. In the current implementation, the required volume of each sample is approximately 20 μL and we measure four samples simultaneously. We demonstrate the performance of the MMR by measurement of the flow curves (viscosity versus shear rate) of three representative polymers: A polydimethylsiloxane melt, a polyisobutylene solution, and a polystyrene melt. We adapt standard data correction methods to account for shear-thinning and entry/flow-front effects. We report a high level of accuracy and precision. This instrument will be particularly useful in cases of multiple samples, limited material quantity, and when optical access is useful. [DOI: 10.1122/1.2955511]

I. INTRODUCTION

Melt rheometry is essential to the polymers industry because it provides critical information regarding the processability of new materials and provides insights into a wide range of fundamental material properties as described in the books written by [Macosko \(1994\)](#) and [Bird *et al.* \(1987\)](#). However, bulk rheological techniques are problematic in cases where material supply is limited, where large numbers of sample measurements are required, and when rapid sample loading and cleaning procedures are needed. For example, in modern combinatorial methods developed by [Takeuchi and co-workers \(2005\)](#), the synthesis of large numbers of new polymers and the fabrication of libraries of polymer blends create severe challenges for rheological characterization.

Two principle classes of rheometers have wide scale use in polymers research: capillary rheometers and rotational rheometers. As described in the book of [Carreau *et al.* \(1997\)](#), rotational rheometers offer the advantage of acquiring dynamic moduli over a range of frequencies, but has the disadvantage of time consuming sample preparation, difficulty of use, large sample size (approximately 500 mg), and of single sample capability. The second type, pressure driven capillary and slit rheometers, is commonly used by industry because it offers simpler measurement protocols and operates at higher shear rates. The primary disadvantages are: Large sample size (approximately 25 g), the fact

^{a)}Author to whom correspondence should be addressed; electronic mail: doyoung.moon@nist.gov

that only one or two samples are measured at a time, and the difficulty of measurement at low shear rates. These two classes of rheometers are thus not amenable to the high throughput approach being developed in many laboratories.

Several methods have emerged recently which enable rheological measurements on significantly smaller samples than had hitherto been possible, although several are not applicable to the high temperature, high viscosity melts of interest here. [Mason and Weitz \(1995\)](#) developed a dynamic method based on the Brownian motion of particles, while [Clasen and Mckinley \(2004\)](#) developed a steady shear method using a sliding plate rheometer with a micro-scale gap separation. [Srivastava and Burns \(2005, 2006\)](#) developed a micro-fabricated nanoliter capillary viscometer in which fluid wicks into micro-fluidic channels and [Aramphongphun and Castro \(2007\)](#) developed a customized micro-slit rheometer using micrometer-sized channel gaps between 25 and 100 μm and a high precision syringe pump.

For polymer melts, [Clay \(2001, 2003\)](#) utilized small diameter parallel plates to quantify the shear rheology of the polymer samples as small as 5 mg. [Mackay \(1991, 1998\)](#) measured the dynamic shear rheological properties of small samples with total volume on the order of 5–25 μL using an attachment for a standard torsional rheometer based on a sliding plate geometry. Considerations regarding the use of standard capillary rheometry but with submillimeter geometries have been discussed by [Benbow and Lamb \(1964\)](#) who considered the range of obtainable stress and viscosity, by [Ybarra \(1980\)](#) and [Hay \(1999\)](#), in terms of the advantageous effects of reduced shear heating and the need to consider pressured induced changes in viscosity. [Shidara \(1993\)](#) described extrudate instabilities and slip. Despite these works, there remains a need for a micro-rheometer which works in parallel on polymer melts over a wide range of shear rates using minimal sample volumes.

Here we present an instrument designed to meet these requirements—termed a multi-sample micro-slit rheometer (MMR)—essentially a pressure-driven slit rheometer. The use of pressure as the driving force allows for simple parallelization of the design as well as mechanical simplicity. The induced flow is measured by optically tracking the position of the flow front as the fluid fills the channel. In our current design, we require approximately 20 μL per sample and measure four samples simultaneously. The MMR offers the simplicity of capillary rheometry and a design that enables parallel measurements on limited quantity samples.

II. APPARATUS

¹The primary design considerations were mechanical simplicity (no moving parts), high temperature capability (materials of construction are stainless steel, aluminum and sapphire), cleanability (no inaccessible cavities), multi-sample capability, and optical access to the fluid. A pressure-driven slit rheometer with miniaturized dimensions can meet these requirements. Figure 1 shows the cross section of the main fixture of the MMR and the main auxiliary components. The heart of the device is the steel shim (standard grade shim stock) which contains four slits through which four independent fluids can flow. The thickness of the shim used here is 132 μm and the slits are 1.3 mm in width and 13 mm in effective viewing length. The shim is sandwiched between a stainless steel sample chamber on the upper side and a disk-shaped sapphire window

¹Certain equipment, instruments or materials are identified in this article in order to adequately specify the experimental details. Such identification does not imply recommendation by the National Institute of Standards and Technology nor does it imply the materials are necessarily the best available for the purpose.

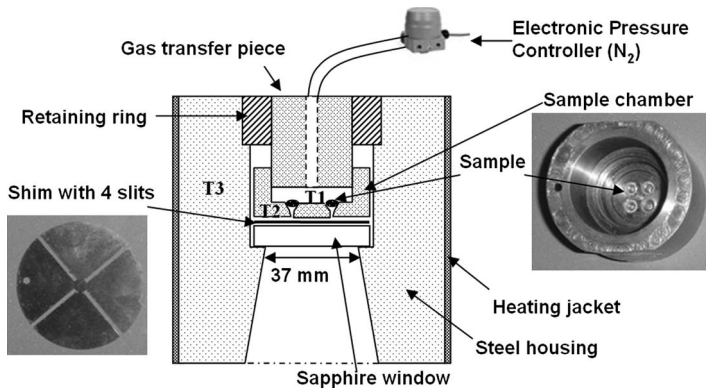


FIG. 1. Schematic diagram of multi-sample micro-rheometer. Pressurized gas drives the fluid from the sample chamber through the slits in the shim. The flow front position is measured as a function of time.

(47 mm diameter \times 5 mm thickness) on the lower side. The samples are loaded into four holes (sample chambers) which are tapered from 4 to 1.3 mm diameters. These holes play the role of the sample holders in a pressure-driven rheometer. When assembled, the four holes are situated directly above the slits at points near the radial center of the window. For the bottom plate, sapphire is used because of its high thermal conductivity (for temperature uniformity across the channels), optical clarity, and mechanical rigidity under applied pressure. The sealing is accomplished simply by a compressive force on the sample chamber-shim-window assembly, carried out by mechanical pressure from the retaining ring on the sample chamber via screws (not shown).

The temperature is controlled through a band heater operating in conjunction with a control thermocouple (T3) and proportional integral differential (PID) temperature controller. We measure the degree of temperature uniformity by placing test thermocouples near the sample holders (T1) and at a point on the sapphire in one of the slits (T2). Over the temperature range from room temperature to 300 °C, T1 and T2 are within 1 °C of each other and T3 exceeds T1 and T2 by no more than 1.5 °C. The time for heating the sample to a typical temperature of 200 °C is approximately 30 min, but this time could be reduced in a future device by utilizing a steel housing with a reduced thermal mass.

For pressure control, nitrogen gas from the regulator of a standard laboratory cylinder flows into a programmable electronic pressure controller (ER3000 series, TESCOM Corporation) and then to the sample chamber. For pressures above 10 kPa, the control is within $\pm 1\%$. For pressure beyond the ER3000 limit of 2100 kPa, the gas simply flows from the regulator to the sample chamber and we recorded the reading of the pressure transducer (Model 68073, Cole-Parmer). Most experiments reported here utilize constant inlet pressure, but we can also apply pressure ramps or more complex profiles.

Upon application of pressure, the four fluids flow down from the sample chamber and radially outward through the four slits, displacing the air. The flow front is imaged by a high-end consumer video camera through a mirror (placed for geometrical convenience.) Proper illumination is critical in order to observe the flow front and we use a fiber optic ring light. The motion of the flow front is analyzed by a commercial motion tracking software (SIMI MatchiX, SIMI Reality Motion Systems) which uses a pattern matching algorithm to track an object as shown in Fig. 2. In the case of constant inlet pressure, the raw position data have an uneven density as a function of time (or length) because the

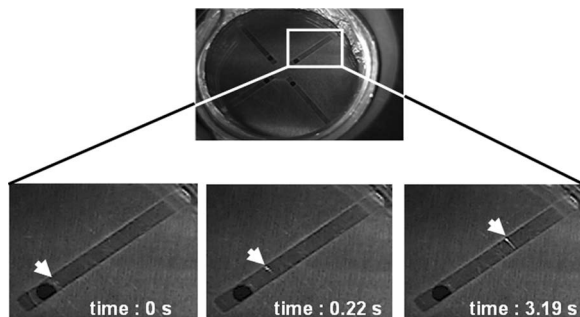


FIG. 2. Motion of a polymer flow front as it is driven through a channel.

fluid slows down as it advances in the slit while the frame rate is constant (30 frames/s). In order to avoid uneven data weighting during the subsequent curve fit, an even sampling procedure is applied to the data.

Three materials are used to demonstrate the capabilities of the device. Two of them are NIST Standard Reference Materials (SRMs): a PIB solution (SRM2490, polyisobutylene dissolved in 2, 6, 10, 14-tetramethylpentadecane) and a PDMS melt (SRM2491, polydimethylsiloxane). Rheological results are reported on them by [Schultheisz and Leigh \(2002\)](#) and [Schultheisz *et al.* \(2003\)](#), respectively. The third is a polystyrene (PS612, DOW Chemical), which is chosen to demonstrate the elevated temperature capabilities. The measured viscosity from the MMR was compared to the reference data for the two SRMs and to the measured results of a capillary rheometer (Rheo-Tester 2000, Goettfurt) for the polystyrene.

The samples are loaded into the sample chamber and allowed to settle so that no bubbles are detected by visual inspection. In the case of polystyrene, two or three solid pellets were loaded in each sample hole and permitted to melt inside the fixture under a nitrogen environment by loosening the gas transfer piece and purging with nitrogen gas to avoid thermal degradation. While not always necessary, a prior step of annealing in a vacuum oven can ensure elimination of gas bubbles from the melt. The experiment is also possible with only one pellet, but for one-half pellet we frequently find that gas bubbles flow through the channel. Consequently with our current design of the sample chamber, the minimum sample quantity of the MMR rheometer is approximately $20 \mu\text{L}$. In the case of the room temperature, the time for melting, disassembly, cleaning and reloading is approximately within 20 min, while for a high temperature melt there is the added time of heating and cooling.

III. THEORETICAL PROCEDURE

A. Basic slit rheometry

We review the basic procedure and assumptions necessary to extract viscosity from the data. We employ several common assumptions: The flow is laminar and sidewall effects can be ignored. In our study, the ratio of height to width is approximately 10, justifying the latter assumption. The schematic diagram of a slit flow channel is shown in [Fig. 3](#). The apparent viscosity can be described by [Eq. \(1\)](#), which is derived in the book of [Agassant *et al.* \(1991\)](#)

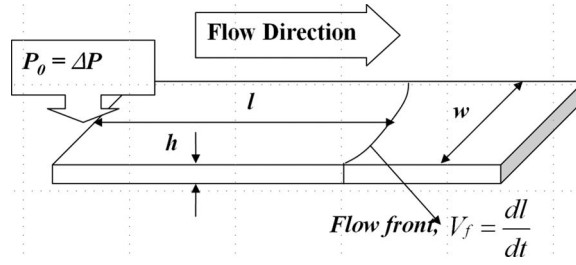


FIG. 3. Geometry of a slit channel.

$$\eta_a = \frac{\tau_w}{\dot{\gamma}_a} = \frac{\frac{h}{2} \left(\frac{\Delta P}{l} \right)}{\frac{6}{h} V_f} = \frac{h^2 \Delta P}{12 l V_f}, \quad (1)$$

where τ_w is the wall shear stress, $\dot{\gamma}_a$ is the apparent wall shear rate, $V_f (= dl/dt)$ is flow velocity of the flow front, ΔP is the pressure drop, h is the slit height, and l is the length of sample in the channel. By measuring the flow velocity V_f at flow length l , the apparent viscosity can be easily obtained from Eq. (1).

The measured data are the flow length l and flow time t , but the flow velocity is needed in order to calculate the viscosity. We apply a 4th order polynomial equation to fit the data with initial boundary conditions $dt/dl=0$ ($dl/dt=\infty$) at $l=0$:

$$t(l) = a''l^4 + b''l^3 + c''l^2 + e'', \quad (2a)$$

where a'' , b'' , c'' , e'' are the fitting parameters. Then, the flow velocity can be expressed:

$$V_f = \left(\frac{dt}{dl} \right)^{-1} = (4a''l^3 + 3b''l^2 + 2c'l'')^{-1}. \quad (2b)$$

The local velocity can also be obtained by a direct method based on a local averaging technique, but this method gives less stable results due to its high sensitivity to local noise in the data. Based on the high-quality fits of Eq. (2a) to the raw data, our curve-fitting approach is justified.

B. Shear thinning correction (Rabinowitsch procedure)

For a shear thinning fluid, slit rheometry also requires a correction in order to obtain the correct wall shear rate, known as the [Rabinowitsch \(1929\)](#) procedure which is summarized in the book written by [Carreau and et al. \(1997\)](#).

In the procedure, the power law index is:

$$n = \frac{d \ln \tau_w}{d \ln \dot{\gamma}_a} = \frac{d \ln \left(\frac{2}{h} \left(\frac{\Delta P}{l} \right) \right)}{d \ln \left(\frac{6}{h} V \right)} = \frac{d \ln(l)}{d \ln \left(\frac{dt}{dl} \right)} \quad (3a)$$

Then, the viscosity becomes

$$\eta = \frac{\tau_w}{\dot{\gamma}_w} = \frac{3n}{2n+1} \eta_a = \frac{3 \frac{dt(l)}{dl}}{2 \frac{dt(l)}{dl} + l \frac{d^2t(l)}{dl^2}} \frac{h^2 \Delta P}{12} \frac{dt(l)}{ldl}, \quad (3b)$$

where η_a is the apparent viscosity. Thus, the Rabinowitsch-corrected viscosity can be obtained according to shear rate as a function of flow length l , flow velocity dl/dt , and its 1st derivative.

C. Correction of entrance and end effect (Bagley correction)

In standard pressure driven rheometry, there is an additional pressure drop due to flow in the entrance and exit regions. Bagley (1957) developed a correction procedure to account for this effect where the pressure drops are measured between experiments in which the flow rate is constant but the channel flow length is varied. By plotting the pressure drop as a function of length and extrapolating to zero length, one can estimate the entrance-exit pressure drop.

We adapt the Bagley procedure for use with the MMR. In place of the flow disturbance due to the exit, we simply consider the flow disturbance due to the leading edge of the flow front. In the present case when flow through a slit is visualized, we do not need multiple die lengths. Instead, the procedure is to run experiments at multiple inlet pressures and then to plot the iso-shear rate curves in the parameter space of pressure—flow length. Each iso-shear rate curve is extrapolated to $l=0$ and the resulting pressure is then the pressure correction. The corrected viscosity can be obtained by subtracting this Bagley pressure from the total pressure at each shear rate.

IV. RESULTS AND DISCUSSION

Figure 4(a) shows the multi-sample capability by plotting the raw data of flow front position versus time. The data for the four channels are nearly coincident for the PDMS demonstrating the uniformity of the four channels. The flow velocity is calculated from Eq. (2b) and plotted in Fig. 4(b). The apparent and Rabinowitsch-corrected viscosity is obtained simultaneously using Eqs. (1), (3a), and (3b) and plotted in Fig. 5. Note that this correction reduces the viscosity, as is well known.

Figures 6 and 7 show an example of the procedure for pressure correction as describe previously. For the PIB solution, a simple quadratic equation is used, so that the pressure correction can be estimated at any arbitrary shear rate. The Bagley correction lowers the viscosity of the PIB solution in the range of the high shear rate (Fig. 7).

Uncertainty in the measurements (see Fig. 8) from the MMR can be evaluated by considering both systematic (Type A) and statistical (Type B) effects. The Type B uncertainty is obtained from repeating an experiment ten times and plotting the variation of results. The uncertainty is less than 5% in the range of $(1-100) \text{ s}^{-1}$. The increased uncertainty at the higher shear rates may be due to several factors. First, the data are obtained when the flow length is still short, and at that position there are the problems of lower sampling data rate, unsteady flow, and the possibility that the data are overly dependent on the exact choice of $l=0$. A major source of Type A uncertainty is the thickness measurement as it gives a second order effect in the calculated viscosity Eq. (1). We estimate uncertainty in thickness to be $2.5 \mu\text{m}$ (manual measurement from a micrometer) translating into a 4% uncertainty in viscosity. The channel height has also been checked by measuring the thickness of a molded polystyrene sample after it has run through the slit and cooled inside the channels. Uncertainty in temperature and pressure

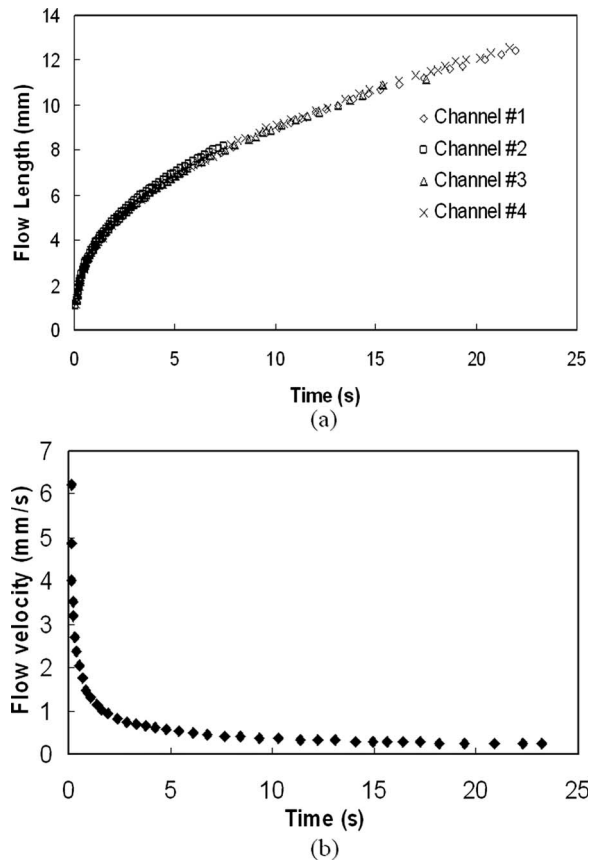


FIG. 4. Flow curves for PDMS (SRM2491) at 23 °C, 1380 kPa. (a) Four channel comparison of flow length versus time. (b) The resulting flow velocity versus time.

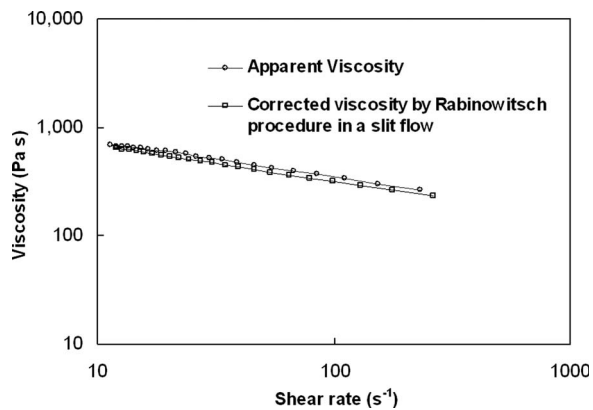


FIG. 5. Correction of viscosity by the Rabinowitsch procedure for the PDMS sample at $T=23\text{ °C}$ and $P=1400\text{ kPa}$.

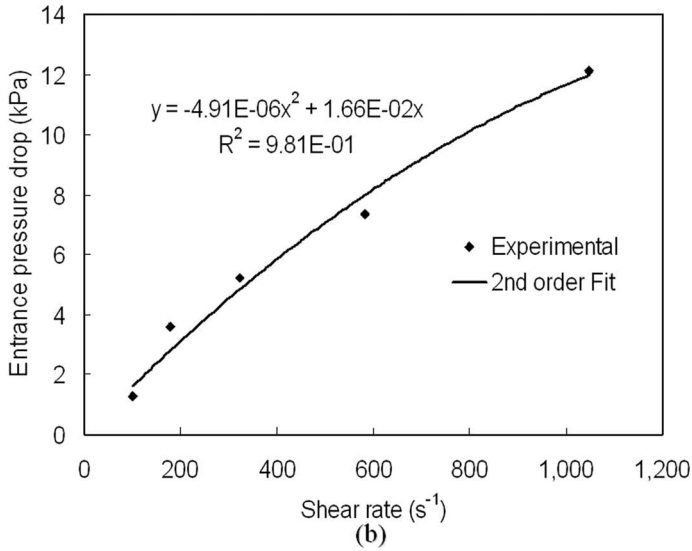
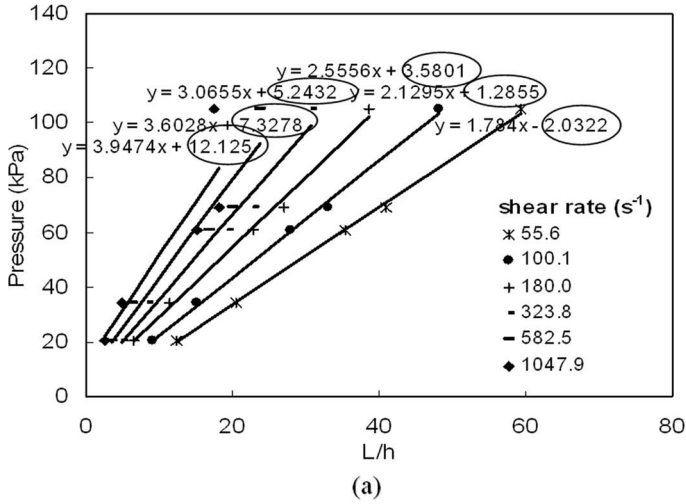


FIG. 6. Procedure for entrance/flow front pressure correction for PIB at $T=24.5\text{ }^{\circ}\text{C}$. (a) Five inlet pressure experiments are conducted $P=(21, 34, 61, 69, 105)\text{ kPa}$. The data points represent the l/h value for which a given shear rate was measured for a given pressure. The solid lines are linear fits to the data—extrapolation to $l/h=0$ gives the Bagley pressure correction. (b) Curve fit to obtain entrance-exit pressure drop for the full shear rate range.

were described earlier. Curve fitting is accepted only for R-square values over 0.999 in our study, and uncertainty from the curve fitting is assumed to be negligible. Consequently, the compounded uncertainty range is (5–10)% for this MMR rheometer design.

Figure 9 demonstrates the overall MMR capability and its current operating window in terms of shear rate, material viscosity and temperature. The lower two data sets show the comparison between the certified and measured viscosity of the PDMS obtained from five inlet pressure experiments (34–2070) kPa, and of the PIB solution (two different inlet pressure experiments) which show good agreement over a wide range of shear rates. The coverage of shear rates in one experimental run of the MMR is approximately one order

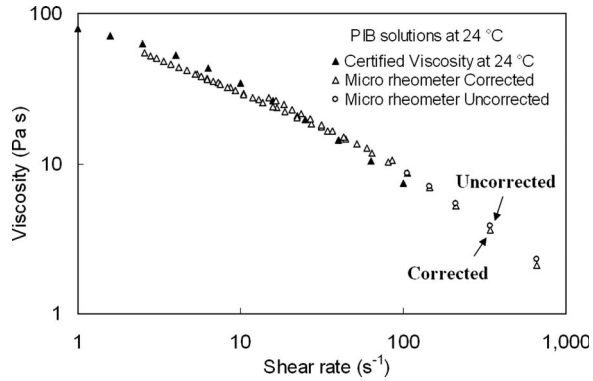


FIG. 7. Results of Bagley correction for PIB at $T=24$ °C. The correction procedure produces a slight decrease in viscosity in the high shear region (>100 s^{-1}).

of magnitude. The result of the polystyrene at 190 °C is compared with that from a conventional capillary rheometer (Rheo-tester 2000, Goettfelt) where the capillary data are obtained from a slit die (depth 1 mm, width 8 mm) for shear rates less than 50 s^{-1} , and from a capillary die (diameter 1 mm) for shear rates greater than 50 s^{-1} . Good agreement between the two measurements was observed as well.

At low shear stress the MMR is limited by the capillarity forces that cause the fluid to wick into the channel. Based on the operating window of Fig. 9, we can say that the current low limit of shear stress is about 500 Pa. The maximum capillary force can be estimated when the surface tension of fluid and channel dimension is known assuming the contact angle is zero (channel perimeter \times surface tension/cross sectional area). In the current MMR channels, the maximum value is about 500 Pa assuming a typical surface tension of 0.03 N/m. The capillarity force can be ignored when the inlet pressure is roughly 40 times greater (~ 20 kPa), a condition met in the reported experiments. Additionally, in the current implementation, when the sample viscosity is less than ~ 1 Pa s, the fluid spontaneously flows into the channel, preventing a controlled measurement.

In addition to the steady inlet pressure experiments described above, one can apply various pressure profiles such as a step-up/down, linear ramp-up/down and even sinu-

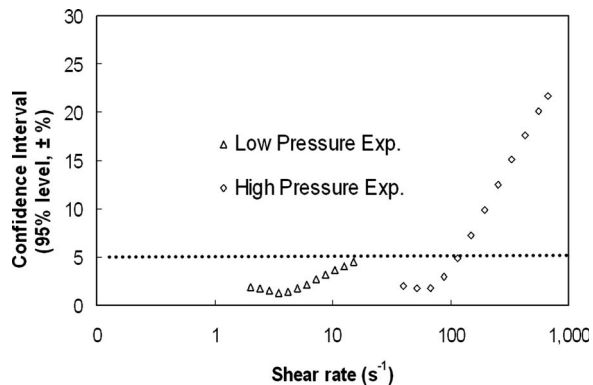


FIG. 8. Analysis of uncertainty based on ten repeated measurements on PDMS at $T=50$ °C and $P=160$ kPa for low pressure or $P=1600$ kPa for high pressure. The uncertainty is below $\pm 5\%$ in the shear rate range from 1 to 200 s^{-1} with 95% confidence level.

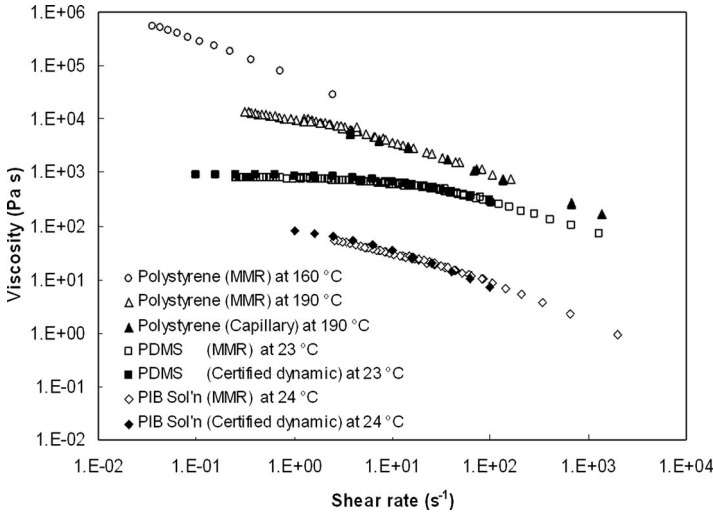


FIG. 9. Summary of the multi-sample micro-slit rheometer’s operating window. Open data points are from the MMR and closed data points are from standard rheometry methods. The Rabinowitsch procedure is applied for all measured results.

soidal profile for the inlet pressure. A linear ramp-up profile can be used to obtain an approximately constant flow velocity (inset of Fig. 10). As the shear rate is steady, the viscosity at this shear rate can be obtained using Eq. (1). Figure 10 shows good agreement with the results of the reference data of PDMS. The steady flow experiment only provides one data point per run, but this test may be important if one is concerned with possible artifacts due to the change of flow velocity during a run. The steady flow experiments are thus complementary to the constant pressure experiments.

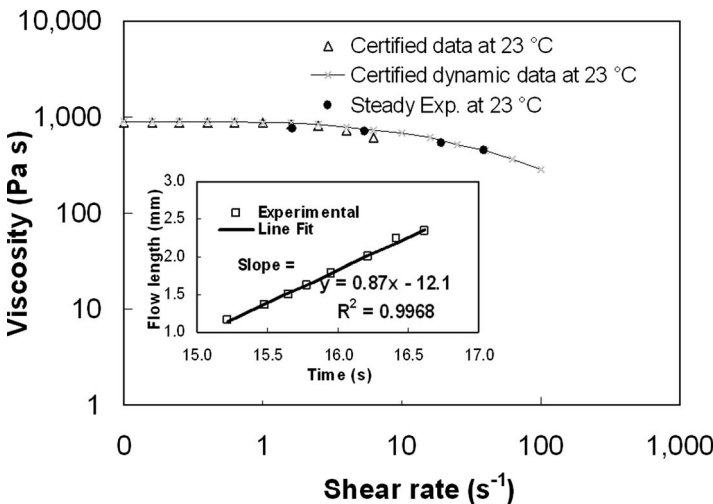


FIG. 10. Results of a quasi steady state experiment obtained by linear ramps of the pressure for the PDMS at $T=23\text{ }^{\circ}\text{C}$. The certified viscosity data are compared to the results of linear ramp experiments at four different dP/dt conditions. Steady state can be verified by the linearity of flow length and time relation (inset).

Although not shown in this paper, we have successfully measured four different materials simultaneously where the maximum difference of viscosity between samples was about two orders of magnitude.

V. CONCLUSIONS AND FUTURE WORKS

Each type of rheometer has an operational window of shear rate, temperature, and viscosity. In this study, we show that the multi-sample micro-slit rheometer (MMR) has a range of five orders of magnitude in viscosity, four orders of magnitude in shear rate (Fig. 9), and operates from room temperature to 300 °C. The MMR has several unique capabilities compared with other macro-scale rheometers such as multi-sample capability, small sample requirement, and micro-fluidic characteristics (flexibility of channel configuration, small size, viewing capability). The MMR data show good agreement with the certified reference data and the results of conventional capillary rheometer, and standard corrections can be applied.

Further, each type of rheometer has inherent weaknesses. In the MMR, once an experimental run is complete, the device must be disassembled, cleaned and reloaded. While these steps are simple, temperature dependent experiments require a new experimental run for each temperature. As shown in Fig. 9 each run covers approximately one order of shear rate but we are working to increase the shear rate range within a single experiment.

We believe that this rheometer is a good choice for applications with limited sample quantity, for high-throughput experimentation, for quality control, and for cases where ease of use is desirable. The operating window can be expanded by changing the shim thickness, by utilizing longer channels, a high speed camera, and pressure controllers that exceed the range (both higher and lower) of the one used here. In order to consider lower viscosity fluids, one needs to explicitly address the contribution of capillary forces to the flow. By changing the shim thickness and increasing the pressure, we believe that the effect of slippage and size dependent measurements can be evaluated. Thus we believe that the MMR fills a need in materials rheometry.

References

- Agassant, J. F., P. Avenas, J. Ph. Sergent, and P. J. Carreau, *Polymer Processing: Principles and Modeling* (Carl Hanser Verlag, New York, 1991).
- Aramphongphun, C., and J. M. Castro, "Microfluidics and rheology of dilute carbon black suspensions for in-mould coating (IMC) applications," *Modell. Simul. Mater. Sci. Eng.* **15**, 157–170 (2007).
- Bagley, E. B., "End corrections in the capillary flow of polyethylene," *J. Appl. Phys.* **28**(5), 624–627 (1957).
- Benbow, J. J., and P. Lamb, "Rheological measurements on polymer melts using very small samples," *J. Sci. Instrum.* **41**(4), 203–205 (1964).
- Bird, R. B., R. C. Armstrong, and O. Hassager, *Dynamics of Polymeric Liquids: Fluid Mechanics*, 2nd ed. (Wiley, New York, 1987), Vol. 1.
- Carreau, P. J., D. C. R. De Kee, and R. P. Chhabra, *Rheology of Polymeric Systems: Principles and Applications* (Hanser Gardner, Cincinnati, 1997).
- Clasen, C., and G. H. McKinley, "Gap-dependent microrheometry of complex liquids," *J. Non-Newtonian Fluid Mech.* **124**(1–3), 1–10 Sp. Iss. SI (2004).
- Clay, J. D., "Melt index from a single pellet," SPE Annual Technical Conference, ANTEC 2001, Vol. 3, 1085–1088 (2001).
- Clay, J. D., "Microrheology and melt index calculations of polymer melts," SPE Annual Technical Conference,

- ANTEC 2003, Vol. 3, 970–974 (2003).
- Hay, G. *et al.*, “Pressure and temperature effects in slit rheometry,” *J. Rheol.* **43**(5), 1099–1116 (1999).
- Mackay, M. E., and C. A. Cathey, “A device to measure the dynamic shear properties of small samples,” *J. Rheol.* **35**, 237–256 (1991).
- Mackay, M. E., *Rheological Measurement*, 2nd ed., edited by A. A. Collyer and D. W. Clegg (Chapman and Hall, London, 1998), p. 635.
- Macosko, C. W., *Rheology: Principles, Measurements, and Applications* (VCH, New York, 1994).
- Mason, T. G., and D. A. Weitz, “Optical measurements of frequency-dependent linear viscoelastic moduli of complex fluids,” *Phys. Rev. Lett.* **74**(7), 1250–1253 (1995).
- Rabinowitsch, B., “Über die viskosität und elastizität von solen,” *Z. Phys. Chem. Abt. A* **145**, 1–26 (1929).
- Schultheisz, C. R., and S. D. Leigh, “Certification of the rheological behavior of SRM 2490, polyisobutylene dissolved in 2,6,10,14-tetramethylpentadecane,” Technical Report No. 260-143, National Institute of Standards and Technology (2002).
- Schultheisz, C. R., K. M. Flynn, and S. D. Leigh, “Certification of the rheological behaviour of SRM 2491, polymethylsiloxane,” Technical Report No. 260-147, National Institute of Standards and Technology (2003).
- Shidara, H., and M. M. Denn, “Polymer melt flow in very thin slits,” *J. Non-Newtonian Fluid Mech.* **48**, 101–110 (1993).
- N. Srivastava, and M. A. Burns, “Nanoliter viscometer for analyzing blood plasma and other liquid samples,” *Anal. Chem.* **77**(2), 383–392 (2005).
- Srivastava, N., and M. A. Burns, “Analysis of non-Newtonian liquids using a microfluidic capillary viscometer,” *Anal. Chem.* **78**(5), 1690–1696 (2006).
- Takeuchi, I., J. Lauterbach, and M. J. Fasolka, “Combinatorial materials synthesis and high-throughput characterization (Invited Review),” *Mater. Today* **8**(10), 18–26 (2005).
- Ybarra, Y. M., and R. E. Eckert, “Viscous heat generation in slit flow,” *AIChE J.* **26**, 751–762 (1980).